energies

MDPI

Article

Impact of Multi-Physics HiL Test Benches on Wind Turbine Certification

Lennard Kaven [1], Anica Frehn [2,*], Maximilian Basler [1], Uwe Jassmann [3,*], Heiko Röttgers [4], Thomas Konrad [1], Dirk Abel [1] and Antonello Monti [2]

[1] Institute of Automatic Control, Center for Wind Power Drives, RWTH Aachen University, 52074 Aachen, Germany; l.kaven@irt.rwth-aachen.de (L.K.); m.basler@irt.rwth-aachen.de (M.B.); t.konrad@irt.rwth-aachen.de (T.K.); d.abel@irt.rwth-aachen.de (D.A.)
[2] Institute for Automation of Complex Power Systems, Center for Wind Power Drives, RWTH Aachen University, 52074 Aachen, Germany; amonti@eonerc.rwth-aachen.de
[3] Conatys GmbH, 52074 Aachen, Germany
[4] Wobben Research and Development GmbH, 26607 Aurich, Germany; heiko.roettgers@enercon.de
* Correspondence: afrehn@eonerc.rwth-aachen.de (A.F.); uja@conatys.com (U.J.)

Abstract: Recently developed nacelle test benches for wind turbines, equipped with multi-physics Hardware-in-the-Loop (HiL) systems, enable advanced testing and even certification of next-generation wind turbines according to IEC61400-21. On the basis of three experiments carried out with a commercial 3.2 MW wind turbine, this paper shows to which extent test bench hardware and HiL systems influence certification results. For the crucial Fault-Ride-Through tests, all deviations were found to be below 1% compared to field and simulation results. For this test, the power HiL system and the accuracy of its impedance emulation are found to be of most relevance. The results for the test items Frequency Control and Synthetic Inertia were found to be more sensitive to shortcomings of the mechanical HiL with its control system. Based on these findings, the paper mentions general procedures to ensure the quality of test benches with HiL systems and, with that, ensure the quality of certification.

Keywords: certification; wind turbine; nacelle test bench; hardware-in-the-loop; grid emulator

Citation: Kaven, L.; Frehn, A.; Basler, M.; Jassmann, U.; Röttgers, H.; Konrad, T.; Abel, D.; Monti, A. Impact of Multi-Physics HiL Test Benches on Wind Turbine Certification. *Energies* **2022**, *15*, 1336. https://doi.org/10.3390/en15041336

Academic Editors: Georg Lauss, Panos Kotsampopoulos and Md Omar Faruque

Received: 30 November 2021
Accepted: 9 February 2022
Published: 14 February 2022

1. Introduction

In the future, the certification of wind turbines' electrical characteristics will heavily depend on measurement results derived on test benches equipped with multi-physics Hardware-in-the-Loop (HiL) systems. Certification measurements on test benches will reduce, and eventually replace, resource-consuming field tests of wind turbines. Currently, Germany already approves the use of test benches for the certification of electrical characteristics by means of the technical guideline FGW TR3 [1]. The technical specification IEC 61400-21-4, which complements the existing standard IEC 61400-21-1 [2], will also make this option available internationally as of 2022 [3]. Both standards allow for the carrying out of Fault Ride Through and Active and Reactive Power Control tests on test benches instead of in the field.

This paper focuses on nacelle test benches as depicted in Figure 1. The setup of a nacelle test bench includes a complete, full-scale wind turbine nacelle with its mechanical and electrical drive train. Thereby, HiL systems operate at the wind turbine's electrical, mechanical, and signal interfaces and enable the operation of the wind turbine as if in the field. While the tower and the rotor are missing, the electrical setup and the control software of the wind turbine remain unchanged.

Figure 1. State-of-the-art multi-megawatt nacelle test bench at the Center for Wind Power Drives, RWTH Aachen University, with an ENERCON E-115 E2 mounted.

HiL systems for nacelle test benches are an active field of research for both academia and the wind industry. Recent publications focus on design aspects of the HiL systems, ranging from different interface methods to control methods that couple a real-time model with the test bench. The effect of different interface algorithms for power-level HiL (PHiL) systems of a wind turbine test bench is investigated in [4]. A similar investigation extended to PHiL simulations in general, and that was not restricted to wind turbine test benches, can be found in [5]. A general method for the selection of an appropriate interface algorithm for PHiL applications is derived in [6]. The authors of [7] use a system identification method to update the knowledge of the hardware and, by this, improve the interface algorithm. To overcome challenges regarding the integration of distributed energy resources, the task-force paper [8] proposes a benchmark system for controller HiL and PHiL testing. For mechanical-level HiL (MHiL), research is more focused on the control of wind turbine test benches. The authors of [9] propose a proportional-integral controller for the emulation of missing inertia on a test bench. A similar approach for MHiL is introduced in [10], but restricted to simulation results for validation. An emulation of rotor inertia and related eigenfrequencies was first introduced in [11], where a state feedback controller shifts the eigenfrequencies of the test bench to the desired locations in the complex eigenvalue plane. The authors of [12] use model-based control, namely an internal model control, and suggest a two-step procedure to design the HiL control algorithm, which also allows eigenfrequency emulation. In [13], a model-based control method damps the test-bench-related eigenfrequencies and applies a reference trajectory. This control method is used to couple a mechanical real-time model for inertia-eigenfrequency emulation in [14]. A similar approach can be found in [15]. This approach controls the test bench's speed control rather than the torque. These control methods have been extended to robust control with a genetic algorithm optimizing the weighting functions used within the controller synthesis in [16], linear parameter varying control where a full-order dynamic output feedback controller adapts to the plant's parameter-varying characteristics [17], and nominal performance in [18].

Most of the aforementioned designs are analyzed in simulation, and only a few were put into operation in full-scale experiments. Full-scale validations with a focus on experimental results are reported in [19] for the initial commissioning of the test bench at the Center for Wind Power Drives at RWTH Aachen University, and in [20] for the electrical faults on the same test bench. In [21], an experimental validation of the rotor eigenfrequency emulation on a full scale test bench is demonstrated, in [22] for mechanical results on the dynamometer at the Fraunhofer IWES, and in [23] for electrical faults on the same test bench. Experimental results, with a focus on the grid emulator, of the wind

turbine testing facility at NREL are given in [24], and practical recommendations regarding the PHiL interface derived from these results are given in [25].

Some of these publications even refer to certification as a possible use case [20,24,26]. However, the specific impact HiL operated test benches can have on certification results has hardly been researched so far, as this is a topic on the fringes of academic interest.

However, the transfer from research results to industrially relevant technology and application requires discussing the impact and limitations that come along with HiL-operated test benches. Hence, sharing experiences made during test-bench-based certification campaigns seems mandatory now and in the future, in order to maintain the high quality of wind turbine certification. While certification on test benches becomes part of the standards, the publicly available data of, and experience with, certification measurement campaigns conducted at nacelle test benches are limited. To the authors' knowledge, only the joint research project CertBench, which the authors were also part of, published such results at all [27]. This project achieved the worldwide first wind turbine certification, solely based upon test bench measurements by means of the German FGW TR3 guideline. An overview of the results [28], and some results on MHiL- [29] and PHiL-specific [30] aspects have been published already.

For the first time, this paper examines, in detail, the impact the HiL system has on certification results. In this way, we try to bridge the gap between the academic perspective on HiL systems and the certification perspective. For this, we investigate how HiL functionalities of a test bench affect the results of selected certification tests and if the observed limitations are significant. This is done by comparing results to field measurements with respect to the evaluation criteria stated in the standards. With that, rather than discussing details of the HiL systems, we focus on the results of certification-relevant measurements. Based on the findings, this paper also aims at deriving procedures which help to ensure the suitability of test benches with HiL systems for certification purpose. The basis for this work is a set of selected results of a measurement campaign carried out with an ENERCON E-115 E2 wind turbine as the device under test (DUT) at the Center for Wind Power Drives and in the field.

The structure of the paper is as follows: Section 2 gives an overview of the general setup of a nacelle test bench before Sections 3 and 4 introduce the PHiL and the MHiL systems, respectively, and discuss their accuracy in an isolated manner. The influence of the HiL systems on the tests Frequency Control, Synthetic Inertia, and Under Voltage Ride Through (UVRT) is discussed in Section 5. Section 6 presents initial ideas on possible validation procedures for HiL-operated test benches.

2. Overview of the Nacelle Test Bench and Wind Turbines

2.1. General Setup and Functioning of a Multi-Physics HiL Nacelle Test Bench

A nacelle test bench with HiL-functionality, as considered in this paper, is comprised of (1) a global test bench control, (2) the DUT (Nacelle), (3) the mechanical-level HiL system, (4) a signal-level HiL system, and (5) the power-level HiL system.

Figure 2 gives an overview of the overall system structure. The global test bench control ensures the safe operation of the test bench and provides an operator interface. The DUT includes the complete drive train with the generator and converter, as well as the unmodified control system of the wind turbine. Compared to a wind turbine in the field, the rotor, the tower, some actuators, and some sensors are missing at the test bench. These elements are reproduced by the different HiL systems. The MHiL system interfaces the DUT's mechanics at the drive train, where the rotor hub is usually mounted, to emulate the dynamics of the missing rotor and to compensate for undesired mechanical effects of the test bench itself. The PHiL system interfaces the DUT's electrical part, provides a medium voltage grid at the point of common coupling (PCC), and allows for the generation of a location-specific grid behavior. As indicated in Figure 2, the MHiL and PHiL systems include real-time simulations, control, and interface software, as well as their actuators motor and controlled PHiL-amplifier (converter), respectively. The signal-level HiL system

emulates the missing sensor and actuator signals and, if required, their dynamic behavior. Thereby, it mainly links simulation in- and outputs to the corresponding in- and outputs of the wind turbine's control system.

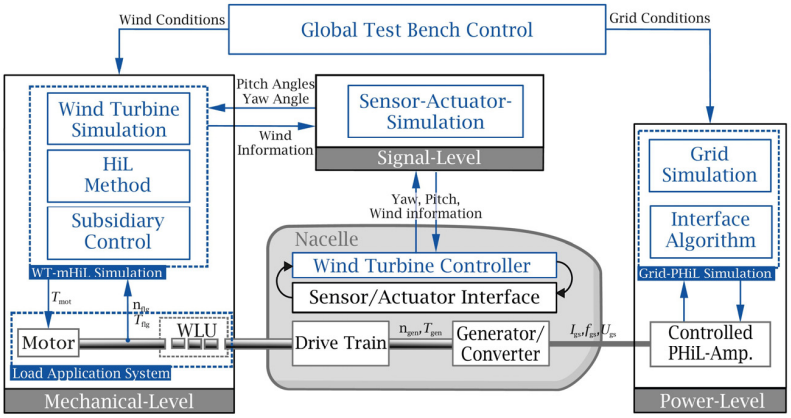

Figure 2. Schematic overview of a wind turbine test bench with multi-physics HiL functionality.

The main purpose of the multi-physics HiL system at the test bench is to enable a realistic operation of the DUT with its original controller configuration under reproducible conditions. For this purpose, the HiL systems have to reproduce the overall system behavior sufficiently accurately to satisfy the DUT's control system and prevent instability [6,9]. If that is not accurate enough, the wind turbine controller would detect mismatches, with the consequence of not being able to operate the DUT. Beyond this, the HiL systems have to be accurate enough to reproduce certification-relevant results from field measurements. For all HiL systems, accuracy must be achieved with respect to: static emulation, dynamic emulation, and the suppression of parasitic effects [6,21]. Table 1 compares what each of these three topics means for the MHiL and PHiL systems. This also emphasizes the cross-domain similarities of the HiL systems.

Table 1. List of tasks and effects for HiL systems and a comparison what they mean in the different domains.

Accuracy	MHiL	PHiL
Static Emulation	▪ Reproducing aerodynamic relations ▪ Emulating missing rotor inertia	▪ Replication of the fundamental frequency component of the grid impedance ▪ Emulating the phase voltages
Dynamic Emulation	▪ Reproducing eigenfrequencies related to missing rotor inertia ▪ Reproducing 3P frequencies	▪ Due to the controller dynamics, the PHiL is only suitable for determining the grid impedances in steady state
Parasitic Effects	▪ Suppress test bench related eigenfrequencies ▪ Minimize impact of actuator limits by adequate controller design	▪ Suppress effects of converter filter, e.g., saturation ▪ Minimize impact of delays via choosing adequate interface algorithm

2.2. Hardware Specification

This section provides some key facts on the hardware specifications of the test bench and the DUT in order to characterize the experimental platform used for this work.

In addition to the real-time simulations of the MHiL and PHiL systems, their associated actuators, the motor, and the converter-based controlled amplifier affect the achievable

accuracy of the multi-physics HiL setup. Other than the HiL simulations, hardware and low-level control algorithms belonging to the mechanical drive unit and the grid emulator cannot be adjusted easily and, therefore, represent hard limits to the performance of the overall system. Table 2 shows the specifications of the nacelle test bench's grid emulator and drive unit. An in-depth introduction to the control concept and the hardware specifications of the grid emulator is provided in [31]. A more detailed discussion on the drive and load unit of the test bench can be found in [32]. With respect to the drive unit, the maximum torque rate represents a crucial limitation to the bandwidth of the MHiL system and its control. In the case of the grid emulator, the switching frequency is a limitation of the PHiL design, both in terms of impedance control bandwidths and harmonic emulation.

Table 2. Specifications of the test bench's grid emulator [31] and drive unit.

	Parameter	**Value**		
Grid emulator	Converter typology	Three-level neutral-point-clamped		
	Max. phase current	3×1100 A		
	Carrier frequency	1150 Hz		
	Transformer windings	Primary	Secondary	Tertiary
	Rated power	8000 kVA	3×2000 kVA	2000 kVA
	Rated voltage	20 kV	3×3 kV	6 kV
Drive unit	Motor type	Direct-drive		
	Rated power	4 MW		
	Rated torque	$\pm$2.7 MNm		
	Max. torque rate	$\pm$1 MNm/s		
	Total inertia (incl. test bench related drive train)	0.51×10^6 kgm^2		
	Manufacturer	General Electric		

The DUT operated at the test bench for this study is a commercially available ENERCON E-115 with a rated power of 3.2 MW. This is a pitch controlled, variable speed wind turbine with direct drive and full-scale power converter. Table 3 summarizes the key facts of the DUT. This is a type 4 wind turbine, where all power is evacuated via the converter, and the generator is almost decoupled from the grid. Therefore, not all findings in this paper may be transferable to type 3 wind turbines, where typically less than 30% of the power [33] is evacuated via the converter and the generator is directly coupled to the grid.

Table 3. DUT parameters based on construction data.

	Parameter	**Value**
Mechanical	Turbine type	Direct drive; variable speed
	Cut-in wind speed	2.5 m/s
	Rated wind speed	13 m/s
	Rotor diameter	115 m
	Share of missing inertia	98.4%
Generator /Converter	Converter type	Full scale power converter
	Generator type	Ring generator
	Rated power	3.2 MW
	Rated generator speed	13.1 rpm
	Wind turbine output voltage	400 V
	Manufacturer	ENERCON GmbH

2.3. Measurement and Uncertainty

All electrical quantities were measured on both the low voltage side of the DUT transformer and the high voltage side. On the low voltage side, the three phase-to-neutral

voltages and the three corresponding phase currents were measured; on the medium-voltage side, the three phase-to-phase voltages and the three phase currents were measured. The instantaneous values were measured with a sampling rate of 10 kHz. A Dewetron DEWE 800 is used as the advanced data acquisition and analysis system. The controlled variable for the control loops within the MHiL system was recorded with an incremental encoder with 2048 pulses per revolution. This sensor is placed on the drive side between the electric motor and the load application unit. All test bench signals used within the MHiL system, such as rotational speed and motor torque as well as the manipulated variable calculated by the MHiL system, are transmitted with 1 kHz. The largest dynamic uncertainty in this setup resulted from the generated power updated at 10 Hz, which inevitably followed from the sample time of the DUT's main control. The aeroelastic simulation model results in the rotational speed and drive torque which then controls the test bench. The systems control reacts to the rotational speed by specifying the generator power (i.e., torque) and pitch angle. These signals are processed in the simulation model and leads to a closed-loop control system. However, the systems control does not directly specify the generator torque and the pitch angle but only the electrical generator power and the pitch rate, i.e., the positioning speed. In order to be able to infer the mechanical acting generator torque for the simulation model from the generator power, a loss model is taken into account and the mechanical torque is calculated with the rotational speed of the DUT. Table 4 summarizes the measurement equipment used.

Table 4. Measurement equipment used.

	Type	Accuracy	Transmission Ratio
Current transducer LV	PEM RCTi-3ph 8000	±1%	8000 A/5 V
Current transducer MV	Chauvin Arnoux Rogowski coils A100	≤1%	200 A/2 V
Voltage transducer LV	Input to the DEWE800	0.01%	
Voltage transducer MV	RITZ VES-24	±1% (80–120%)	20,000/110 V

3. Introduction of Power-Level HiL System

This chapter gives details on the PHiL system and discusses the possibility of impedance emulation in case of faulty grids. For this, the PHiL system is considered in an isolated manner, without considering certification-relevant tests.

3.1. Power-Level HiL Setup

Testing under laboratory conditions requires the mapping of different grid parameters. In addition to the voltage level and the grid frequency, these also include the grid impedances, since they affect the measurement of the electrical properties of wind turbines, which is necessary for certification. The grid impedance should be separately adjustable according to amplitude and grid angle [34]. Since the evaluations of the measurement results required for certification usually refer to the fundamental frequency components, it is also sufficient to specify the 50 Hz component of the grid impedance [1,2].

The grid simulation implemented at the nacelle test bench serves as impedance control, which is part of the grid emulator. This is implemented as a PHiL setup. Input parameters of the real-time grid simulation are the current controlled by the WT (I_{DUT}), which is measured at the PCC, and the specified grid impedance (Z_{Grid}). Using these parameters, the grid model, whose simplified equivalent circuit is shown in Figure 3b, calculates the voltage difference across the grid impedance and adds it to the specified grid voltage (U_{Grid}). The voltage determined in the grid simulation (U_{PCC}) is the new set-point of the grid emulator, which now operates in an impedance-controlled manner. The corresponding structure of the grid emulator, consisting of the real-time measurement, the control, and the hardware components, is shown in Figure 3a [35].

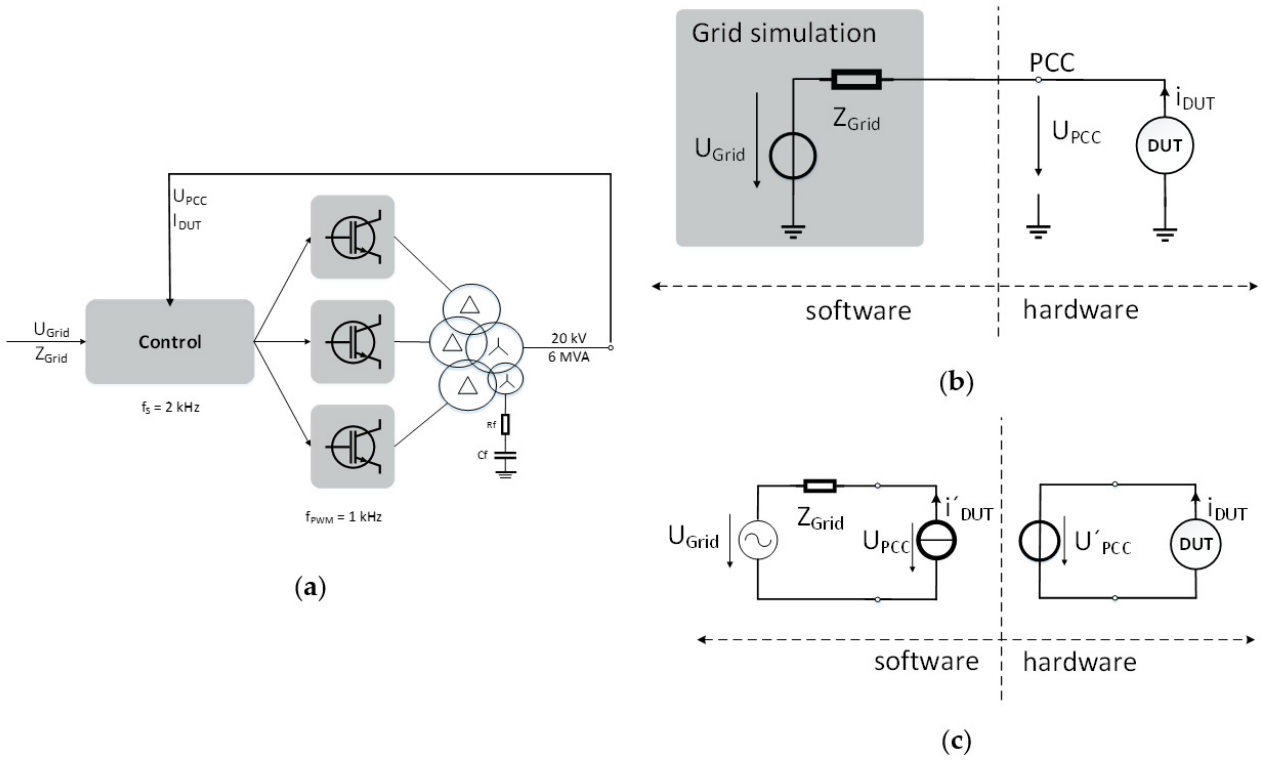

Figure 3. Overall power-level HiL Control Concept [35]. (**a**) Impedance control implementation as part of the grid emulator, (**b**) Single-phase equivalent circuit, and (**c**) PHiL implementation using an ITM interface algorithm.

The single-phase equivalent circuit in Figure 3b illustrates the real-time grid simulation in the left part, and the available hardware as DUT in the right part. Thus, a transfer of the equivalent diagram into a PHiL setup is possible. Figure 3c represents the transfer using the ideal transformer model (ITM) [5,6] as an interface algorithm.

3.2. Impedance Control during Grid Fault

In a former publication, we have already shown that the impedance control provides precise results in steady state operation [35]. This work investigates to what extent the PHiL setup allows an impedance replication in case of faulty grids, e.g., in case of under-voltage events. The impedance is evaluated only for the steady state and for the quasi-steady state fault. The transient transition from the pre-fault to the fault condition occurs in such a short time step that the control of the grid impedance is not operative due to the limited bandwidth of the control loop. Instead, the physical impedance of the installed components is leading during this highly dynamic transition. Since the impedance of the DUT's transformer affects the resulting impedance, it must be considered when evaluating PHiL simulation under steady state conditions. Thus, the total impedance is obtained by adding the transformer impedance and the impedance implemented in the real-time simulation. The impedance, calculated from the current and voltage measurements, is compared with the impedance set point for three-phase UVRT tests with 0.5 pu residual voltage (see Figure 4). The tests were performed under full load (FL) and partial load (PL) conditions of the DUT. In the partial load case, additional measurements considered different reactive current injections, Δi_B. The *k*-factor defines this reactive current injection as a function of the voltage dip depth, Δu [36].

$$\Delta i_B = k \cdot \Delta u \tag{1}$$

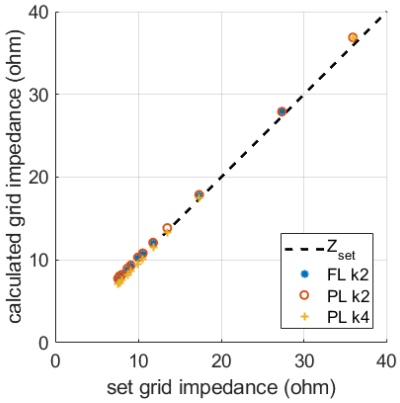

Figure 4. Set and measured grid impedance magnitude.

The evaluation in Figure 4 indicates deviations of less than 1 Ohm between the set values and the values of the grid impedance calculated from the measurements. Thus, UVRT tests with different grid parameters, i.e., grid impedances, can be performed on the grid emulators, if a PHiL system emulates the impedance.

In addition to the impedance magnitude, the impedance angle can also be specified. For this purpose, the X/R ratio is varied. To investigate the behavior in a faulty grid again, three-phase UVRT tests with 0.5 pu resulting voltage at variable X/R ratio were performed, as in the previous investigation. Figure 5 shows the angle variation for a weak grid with 14 MVA short-circuit power (S_{SC}) and a strong grid with 228 MVA short-circuit power. Further tests with short-circuit power between these two values confirm that the deviations decrease with increasing short-circuit power. The maximum deviation at 14 MVA is 2.7°.

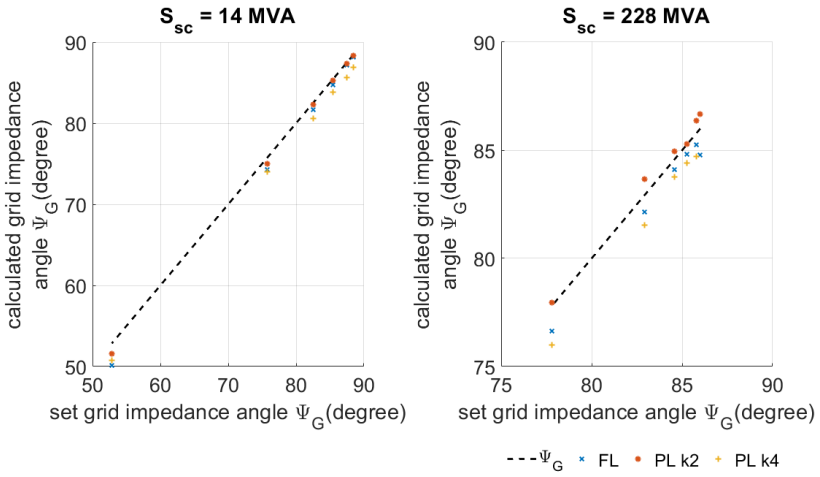

Figure 5. Calculated and measured grid impedance angle.

Thus, the impedance control of the PHiL system enables the specification of different impedance magnitudes and impedance angles during the steady state and quasi-steady state of a UVRT event.

4. Introduction of the Mechanical-Level HiL System

Equivalent to the previous chapter regarding the PHiL system, this chapter describes the MHiL system before the static and dynamic properties of the system are discussed.

4.1. Mechanical-Level HiL-Setup

The MHiL system consists of a wind turbine simulation for reference generation, including aerodynamic and mechanical real-time models (c.f. Figure 6) and control-loops for reference tracking. The aerodynamic model calculates an input torque to the mechanical

drive train of the wind turbine according to user-given wind conditions, rotor blade pitch, and the measured rotation speed. The wind turbine simulation outputs a reference value to the tracking control, which operates the test bench's drive unit.

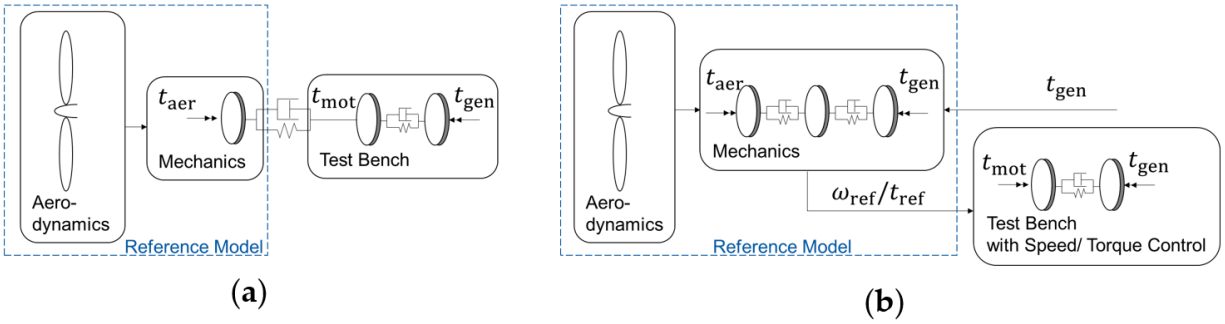

Figure 6. Mechanical-level HiL methods: Inertia Emulation (**a**) and Model Reference Control (**b**).

In this chapter, two different MHiL methods are considered: Baseline Inertia Emulation (IE) [9] and Model Reference Control (MRC) [21]. In the IE, the mechanical model only consists of the rotor inertia and does not include the generator's share, which exists at the test bench. This mimics a flexible connection of the simulated inertia to the DUT at the test bench as depicted in Figure 6a. Due to its simplicity, this method is particularly suitable for commissioning HiL systems in a time-efficient manner [37]. In contrast, the MRC HiL method features a complete wind turbine model, also including the generator's inertia as shown in Figure 6b. The generator speed is the reference value for the tracking control. Due to a large number of parameters, this method offers greater potential in terms of closed-loop robustness and performance. However, this is also accompanied by an increased commissioning effort compared to the IE [21].

4.2. Accuracy of MHiL during Normal Wind Turbine Operations

4.2.1. Stationary Accuracy during Normal Power Production

In this section, the stationary accuracy of the MHiL system is assessed by looking at the power curve of a wind turbine. The measurements are derived by operating the DUT in turbulent wind conditions at different power levels. To calculate the power curve at each level, a 10-min power average is calculated. Therefore, we consider this measurement to be stationary accurate. This curve is an excellent measure to assess the MHiL system accuracy, as it is directly linked to the mechanical quantities of speed and torque, which are controlled by the MHiL system.

Figure 7 shows the nominal power curve from the data sheet (blue line), the power curve derived in a field measurement campaign (gray dots), and the curves derived at the test bench with the two MHiL methods introduced before (orange and purple dots). The field-power curve shows the typical scattering of 10-min power bins caused by inhomogeneous wind conditions. Since the wind speed in the field can only be measured at certain points, identical average wind speed values do not guarantee identical wind conditions over the entire rotor area. This causes the scattering of the measured power.

The artificial wind fields within the MHiL system ensure that the statistical properties are correct over the complete rotor area. This leads to minimal scattering for 10-min average power values derived with artificial wind fields of identical statistical properties. At the same time, this does not mean that the measurements derived at a test bench must match the theoretical blue power curve, as there are other effects, such as losses of the real physical components and other measurement uncertainties, which can lead to a difference of several percent. From the authors' experience, the MHiL system can be considered to be stationary accurate when the deviation from a provided power curve is within the scattering typically observed in the field. Both the IE and the MRC results in Figure 7 are located within this scattering. The difference between the theoretical power curve and the MHiL results is

always below 0.1 pu, which is considered acceptable. At the same time, for both methods, repetitive tests lead to differences in the results of less than 0.02 pu and are well beyond any reproducibility in field measurements.

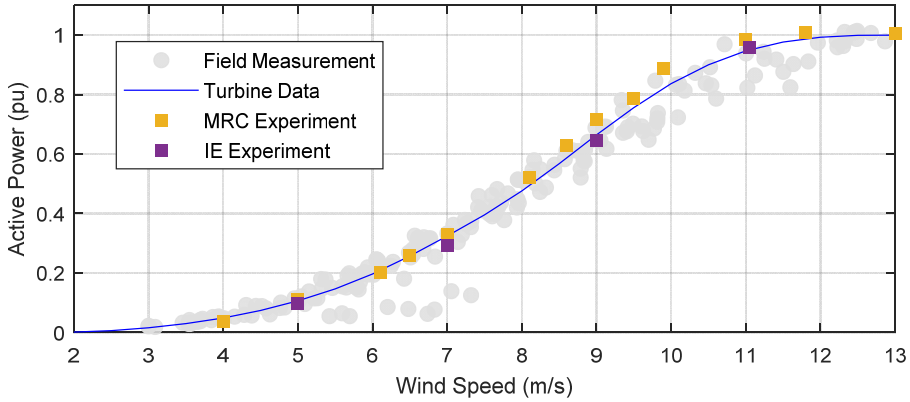

Figure 7. Power curve of the tested wind turbine derived at the test bench with the Inertia Emulation Method and Model Reference Control, in the field and from the turbine's data sheet.

4.2.2. Dynamic Accuracy during Normal Power Production

The dynamic accuracy of the MHiL system addresses its ability to reproduce the mechanical eigenfrequencies of the coupled rotor drive train system. These eigenfrequencies can be found in the spectrum of the drive train's rotation speed and, hence, in the active power. A 10-min power measurement taken during normal operation is considered for analysis. As explained before, the wind speed in the field and in the simulation cannot be identical, which explains the two different wind speed curves in the top plot of Figure 8. The average of both is 15 m/s. The second and third plot in Figure 8 show spectra of the active power when the MRC and the IE are used at the test bench. The MRC is able to emulate the lowest two frequencies and, to a certain extent, also the highest relevant eigenfrequency at approximately 2 Hz. The IE only emulates the first and a minor second frequency.

The emulation's accuracy of both methods is high in terms of frequency and amplitude with respect to values in the low frequency range. The higher frequency emulated by the MRC differs by 9% from the frequency value observed in the field. The power captured within the emulated frequency is only 25% of the field result. The root cause for this is the turbine simulation model within the MHiL system, which itself differs from the field results. As the bottom plot in Figure 8 shows, the results of the MRC method at the test bench match the results of the internal mechanical model. This means that the MRC method operates accurately. The difference emphasizes the importance of accurate wind turbine models, since test bench results cannot be better than such. The accuracy of such models is generally high, as they have been validated for several years and with several wind turbine types. It is not expected that the accuracy of such models gets worse due to increasing wind turbine size. Still, regular and comprehensive validation is mandatory to ensure the model quality.

In conclusion, the accuracy of the MRC method is higher than the IE method, with respect to the nominal frequencies reflected by the internal model, but low with respect to the field results, due to a model mismatch. Consequently, the MRC method is used for subsequent tests. However, with respect to electrical certification, especially active power, one must admit that the power share within the emulated frequencies is low compared to the DUT's nominal power, so that both methods allow realistic testing of type 4 wind turbines.

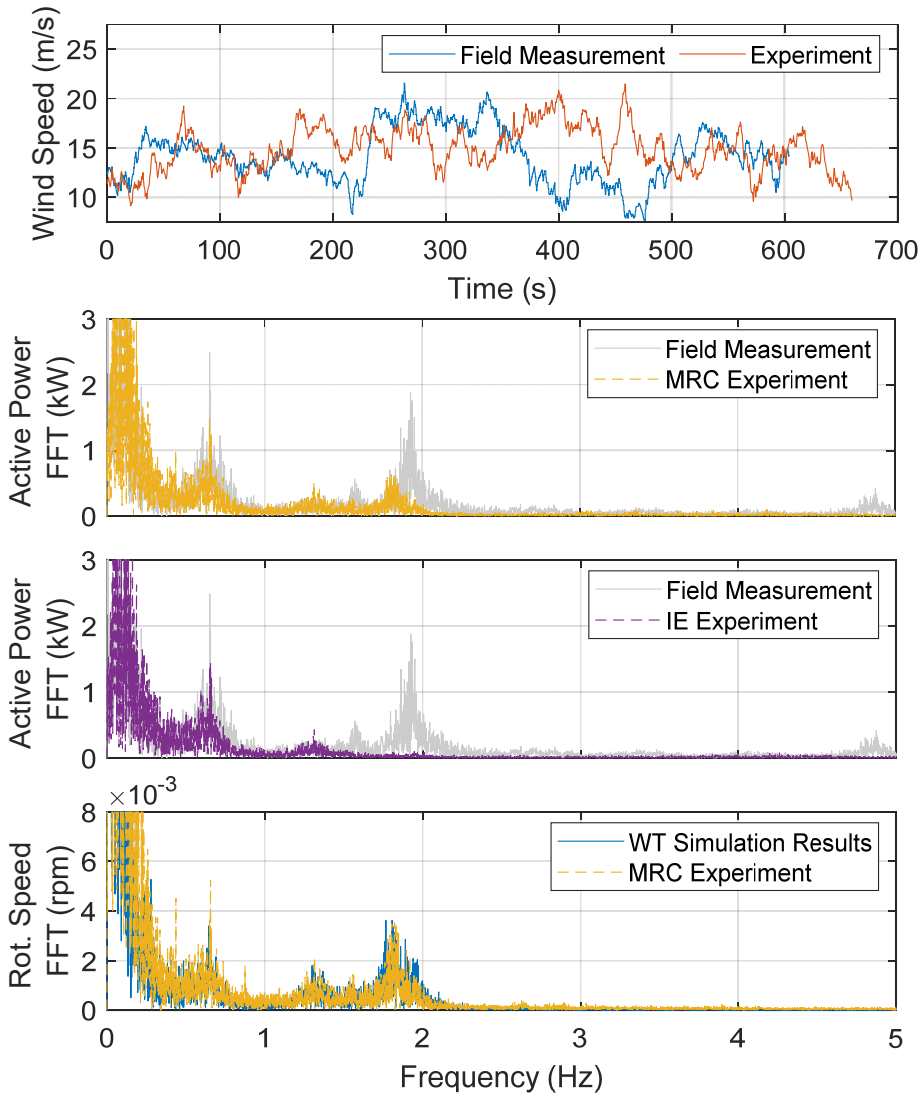

Figure 8. Frequency analysis of the active power output during normal operation of the DUT in the field and at the test bench.

5. Analysis of the HiL Systems' Impact on Selected Certification Tests

This chapter describes the HiL systems' reaction during selected certification-relevant tests and discusses their influence on the measurement and, hence, the certification results. For this purpose, three different tests from IEC 61400-21-1 are considered. These are Under Voltage Ride Through (UVRT) events, Frequency Control, and Synthetic Inertia.

The UVRT event is one of the most important tests when it comes to certification and one of the main reasons for test-bench-based certification for the industry. The influence that the MHiL has on the measurement results is expected to be minor because the DUT is a full-scale power converter wind turbine, so the mechanical drive train and the electrical grid are not coupled directly. The impact of the PHiL system on the test results is expected to be more significant, as the emulated impedance determines how the grid voltage reacts on the wind turbine's reactive current injection and, hence, the course of the test.

Beyond that, this chapter discusses Frequency Control and Synthetic Inertia tests. For both tests, the MHiL system can have a more significant influence on the measurement results because the tests include major and rapid active power changes. The PHiL system was not found to influence these test results in any form and is, therefore, not discussed for these tests.

5.1. Under Voltage Ride through Events

This section investigates the influence of the PHiL and the MHiL system, respectively, on the UVRT results in comparison to field measurements.

5.1.1. PHiL Impact on UVRT

Testing the UVRT capability of a wind turbine in the field usually requires a voltage-divider-based test device. Both IEC 61400-21-1 and FGW TR3 recognize the voltage-divider-based test equipment as state of the art and describe their functionality in more detail. During UVRT tests carried out with such a test device, the impedance at the PCC of the DUT changes with time [38]. Before the actual fault is generated, a series impedance is switched into the circuit, while during fault generation an additional shunt impedance (also called short circuit impedance) is active. In order to show the extent to which the impedance control on the grid emulator enables the reproduction of state-of-the-art field results with a voltage-divider-based test device, an experimental series with two-phase UVRT tests is carried out. In a first measurement sequence, the real-time simulation of the PHiL setup maps the grid impedance and the series-connected impedance of the voltage-divider-based test equipment. In a repetition of the test sequence, the real-time simulation additionally includes the parallel connection of the shunt impedance. Subsequently, these measurements are compared with field data of an identical DUT type.

Figure 9 shows the comparison of the positive and negative sequence voltages determined from the field measurement and from the grid emulator running a PHiL simulation. The example measurement is a two-phase UVRT test to 0.25 pu residual voltage. For the results in the upper diagram, the PHiL simulation only includes the series impedance, while for the results in the lower diagram, it also simulates the shunt impedance. The exclusive representation of the series impedance in the PHiL simulation leads to a deviation of 4% in the positive sequence voltage. The negative sequence even shows a deviation of 8%. This deviation decreases to less than 1% if the PHiL simulation includes the shunt impedance in addition to the series impedance (Figure 9 bottom).

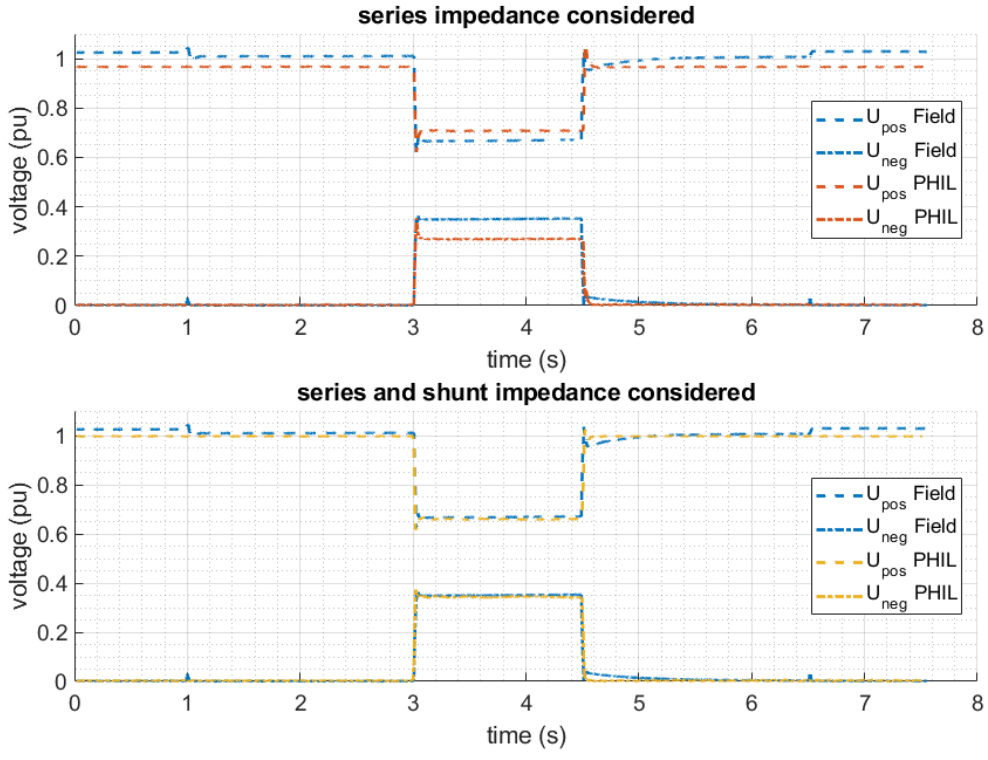

Figure 9. Comparison of the positive and negative sequence voltages between a field and a grid emulator measurement using the PHiL setup.

In order to assess the performance of the DUT, Figure 10 compares the reactive current injection for voltage support observed in the field and at the test bench. Again, the DUT shows identical characteristics on the test bench as in the field, provided that the real-time PHiL simulation maps the shunt impedance in addition to the series impedance of the test equipment. If only the series impedance is simulated, the deviation of the reactive current injected into the positive sequence system increases to 13%, while it is 10% in the negative sequence system. This example shows that by emulating the voltage-divider-based test method's impedance in the PHiL simulation, the test bench is capable of reproducing field characteristics. This is even correct when the PHiL simulation does not emulate the switching of the impedances through the course of the test, but keeps the impedance constant at the impedance level required during fault generation, as well as before, during, and after the fault.

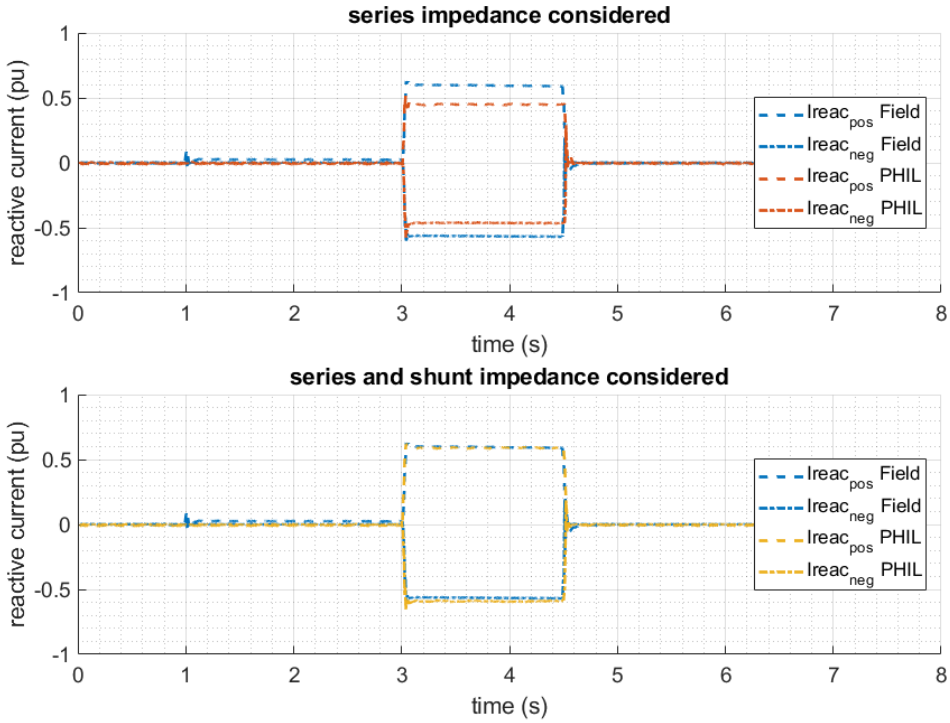

Figure 10. Comparison of the positive and negative sequence reactive current between a field and a grid emulator measurement using the PHiL setup.

For a more comprehensive comparison over different operating points, Figure 11 shows the calculated positive and negative sequence voltages for all tested voltage dip depths of the two-phase UVRT tests. Except for the dips <0.05 pu, all dip depths result in discrepancies of less than 1% between the field measurement and the test bench measurements that include series and short-circuit impedances in the PHiL simulation. For the <0.05 pu tests, a resulting voltage of 0.02 pu was set on the grid emulator, while this was 0 pu in the field. The different setting ultimately results in a 2% deviation. The differences between the measurements that include the shunt impedance and those that simulate only the series impedance is up to 0.15 pu in the positive sequence. This deviation decreases to 0.01 pu when the residual voltage increases to 0.73 pu. This is because of the decreasing discrepancy between the resulting impedances. The difference between the shunt and series impedances is 7.52 ohms for a residual voltage of 0.73 pu, while it is 28.55 ohms for a dip to 0 pu.

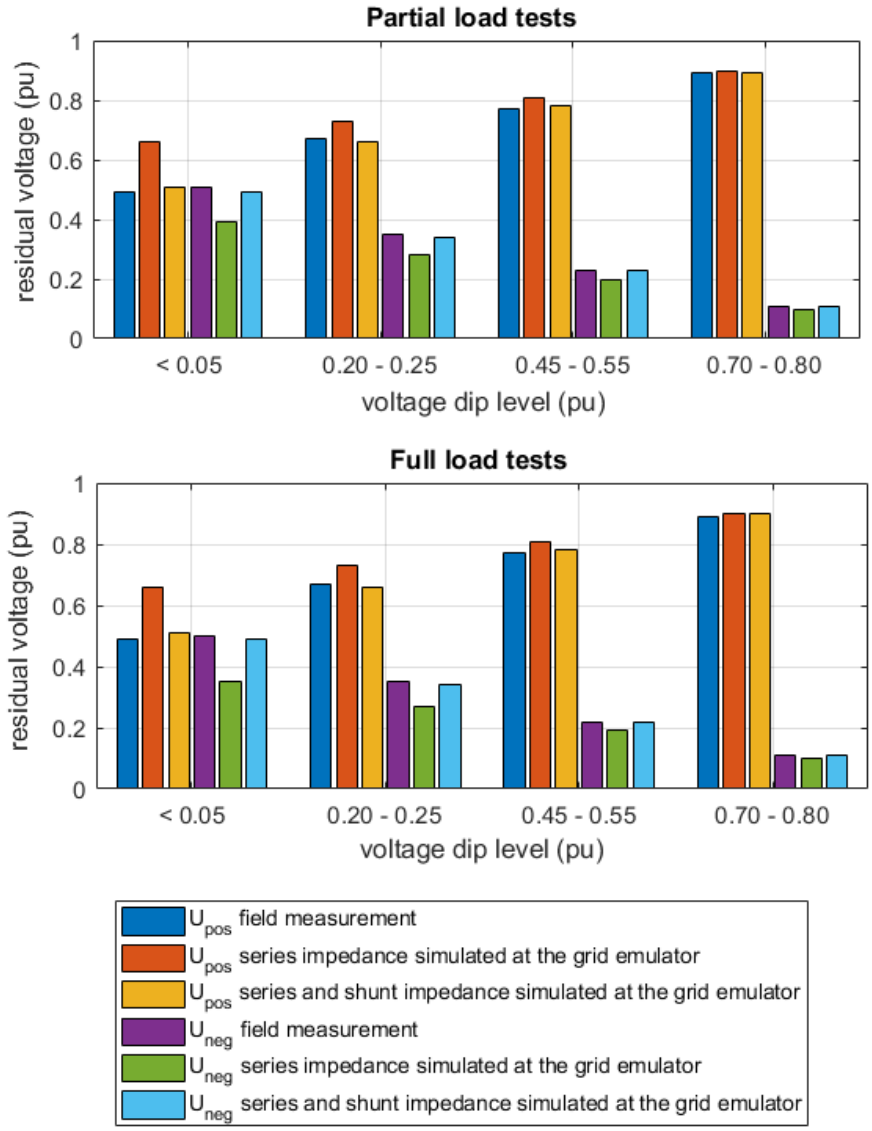

Figure 11. Direct comparison between field measurements and grid emulator measurements using the PHiL setup.

In conclusion, the DUT's reactive current injection shows identical results for field and bench tests, as long as the real-time simulation of the grid impedance simulates both the series and shunt impedances of the voltage-divider-based test equipment.

5.1.2. MHiL Impact on UVRT

This section discusses the role the MHiL plays for an UVRT event tested at a test bench. Since the DUT is a type 4 wind turbine and equipped with a full-scale power converter, grid events are very much decoupled from the mechanical system and, hence, from the MHiL system. For type 3 wind turbines without a full-scale power converter, a much more significant interaction is expected.

To illustrate, how the MHiL reacts to a grid fault event, a three-phase voltage dip to 0 pu in partial load is chosen. Many other symmetrical and asymmetrical voltage dips with different residual voltage levels and different X/R ratio were tested and, in principle, lead to identical results. Figure 12 shows the mechanical quantities of the DUT during the UVRT event, such as wind speed, pitch angle, various torques, rotor speed, and active power, calculated from measured current and voltage. Figure 13 shows the corresponding measurements for voltage, active current (I_{act}), and reactive current (I_{reac}). As the top plot

in Figure 12 shows, the test was carried out at a constant wind speed. The bottom plot in the same figure features the active power, calculated at low- and medium-voltage, and indicates that the UVRT event begins at 60 s and lasts 400 ms, which can also be observed in the voltage plot in Figure 13. For assessing the MHiL's impact, the speed values in Figure 12 are of interest. Before the fault begins, the MHiL internal speed reference and the measured generator speed at the test bench match. As soon as the fault occurs, the actual generator speed differs from the reference speed set by the MHiL. The observed acceleration is caused by a drop of the generator torque at the fault occurrence. It takes the MHiL system approximately 1 s to control the generator speed oscillation and up to 2 s to reduce the control error significantly. In the moment when the generator torque drops, the DUT and the reference model change their rotational speed according to their inertias with approximately 0.045 pu/s and 0.00054 pu/s, respectively. This acceleration of the DUT corresponds to a 0.01 pu (24 kNm) drop of mechanical generator torque, which matches the generator torque drop in Figure 12 (22 kNm). This generator torque, calculated from electrical power, does not drop immediately, but after a delay time of 0.11 s, whereas the mechanical generator torque drops after 0.02 s, indicated by the DUT acceleration. This delay time of the calculated generator torque, which is an input to the MHiL system, contributes to the observed deviation. However, the maximum deviation of the reference and the measured speed is less than 0.5%. During all UVRT tests, no deviation of the MHiL reference and measured generator speed higher than that was found.

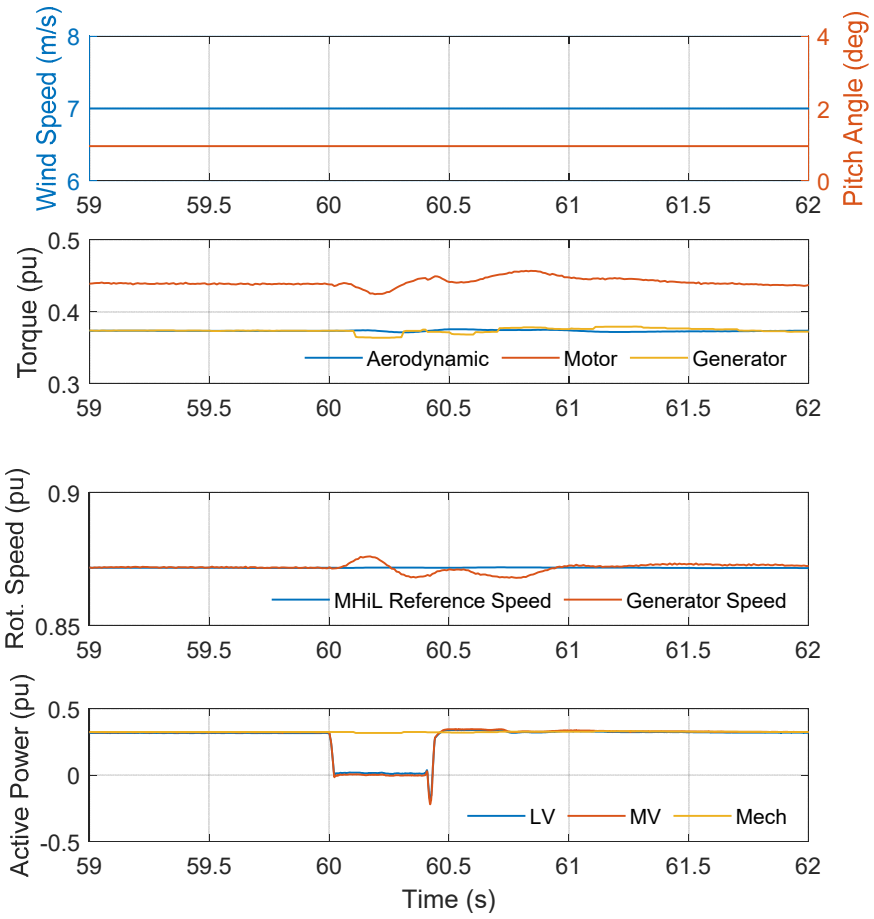

Figure 12. Mechanical quantities for 3 phase 0 pu UVRT in partial load.

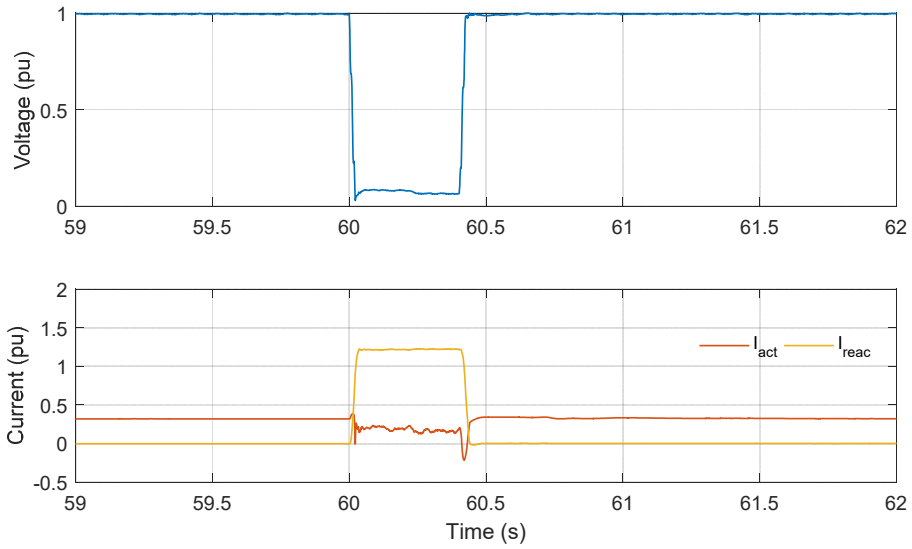

Figure 13. Voltage and currents during UVRT on the low-voltage side.

As the rotation speed and torque are linked to active power, an influence of the MHiL system on the certification results would be expected only in the active current or power measurement. As the bottom plot in Figure 12 shows, no significant impact can be found.

In conclusion, there exists a minor interaction between the grid fault and the mechanical quantities. The analysis shows that the occurring deviation of the rotation speed, controlled by the MHiL system, does not influence the certification-relevant quantities negatively. However, for type 3 wind turbines, such a deviation may have relevant consequences, which is why the issues with the speed deviation should be resolved.

5.2. Frequency Control

With the Frequency Control test, the DUT's ability to reduce active power output in the case of over-frequency is tested. An increased grid frequency indicates a power surplus in the grid and leads to a power drop of the DUT. A lookup-table, implemented in the DUT control, specifies the relationship between power and frequency. The limitations for power change-rates are set as high as possible when decreasing power. The power increase is subject to change-rate limitations. In the certification, the resulting static active power is considered by the IEC 61400-21-1 standard. The German FGW TR3 standard also analyses the dynamic transition, i.e., settling time, of the power. As the desired behavior requires rapid changes of the wind turbine's active power, the rotor emulation of the MHiL systems plays a crucial role. An impact of the PHiL system was not observed, and is thus not discussed further.

A comparable test with the same DUT, but at a different test bench with another MHiL system, was presented in [29]. The results presented therein are very promising in terms of the MHiL system's performance. Different from this work, discussing the influence of the MHiL on the results was not the focus of that paper and of less relevance, due to high MHiL performance.

At the nacelle test bench, the test was executed with laminar wind. According to the German standard FGW TR3 Rev. 24, the frequency varies from 50 Hz to 50.25 Hz, 50.7 Hz, 51.15 Hz, and 50.07 Hz, before it is set to the nominal 50 Hz again. Each frequency level is held for 30 s. Figure 14 shows wind speed, pitch angle, several torques, generator speed, and active power for the complete test procedure. On a macroscopic scale, the DUT power reacts as expected, with a power decrease and an increase when the frequency rises or falls, respectively. In more detail, the MHiL internal signals' reference speed and actual speed show relevant deviations during dynamic transitions between 75 s and 110 s. The deviation is up to 4%.

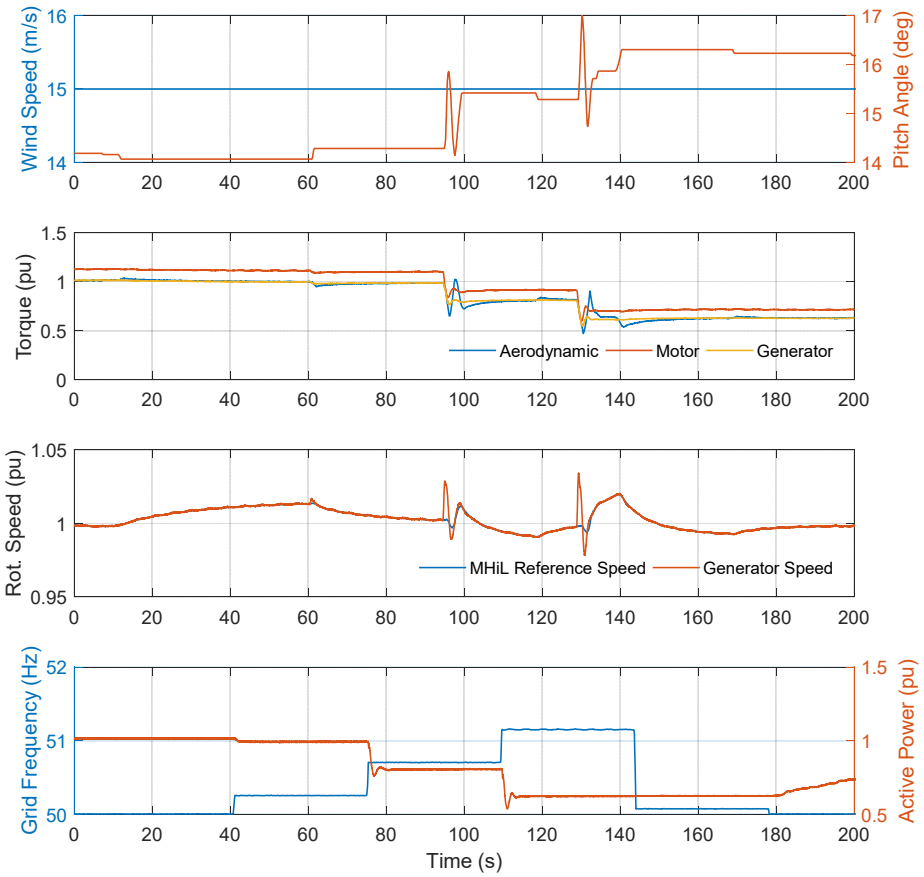

Figure 14. P(f) test according to TR3 Rev. 24.

At 75 s, the frequency increases from 50.25 Hz to 50.7 Hz and causes the DUT to rapidly reduce its active power output. This decrease leads to a lowered generator torque and an undesired generator speed increase at the test bench. In the field, the immense rotor inertia of a wind turbine prevents this. At the test bench, the MHiL system should reproduce this impact of the inertia. As described in the previous chapter, the delay of the generator torque signal and the limited control bandwidth prevent an adequate reaction of the MHiL system. This is due to a motor torque change-rate limitation, which is used up by approximately 80% during this test. Since the MHiL is designed such that the maximum is not fully exploited for robustness reasons, the observed shortcoming is linked to that test bench limitation.

Another effect which influences the MHiL performance is the interaction of the MHiL control with the DUT control. Due to the MHiL's limited bandwidth, both controls are not fully decoupled in the frequency range and interactions may lead to oscillations. This theory is supported by the fact that the pitch angle, commanded by the DUT control, reacts in accordance with the observed speed oscillations. The interaction of both controls acts similar to a positive feedback. The increase of the generator speed increases the power for a given torque, instead of decreasing. Consequently, a further reduction of the torque is commanded by the DUT, which, in turn, lets the generator accelerate and so on. Both the MHiL and the DUT's speed control try to level the input torque to the same level as the generator torque, but interfere with each other when trying so. After a settling time of 5 s, the tracking recovers.

The presented issues do not influence the steady state power, i.e., the settled power after 30 s. Since the IEC 61400-21-1 only considers this, the certification outcome would be unchanged. Only with respect to the settling time, which at least the German FGW TR3 considers as certification criteria, the result does affect the certification. This leads to a stated performance in a turbine certificate, which is worse than it is in reality. While

this may be acceptable from a certification point of view, since the results would be more conservative, it is not desirable for the manufacturer to misrepresent the product as being worse than it actually is.

5.3. Synthetic Inertia

In contrast to the Frequency Control test, the Synthetic Inertia test evaluates the DUT's ability to provide additional power to the grid in case of an under-frequency event [2]. The test must be carried out at different power levels, namely between 0.25 and 0.5 pu, 0.8 pu, and 1 pu. For how long a wind turbine must be able to provide additional power depends on the DUT specification and is not defined by IEC 61400-211.

In this paper, we discuss a measurement at 1 pu power, with turbulent wind conditions carried out at the test bench. Figure 15 shows wind speed, pitch angle, several torques, generator speed, grid frequency, and power. At 6 s, the grid frequency decreases stepwise to 48.5 Hz and recovers to 49.3 Hz at 15 s. After the grid frequency drops, the power boost phase, where the power is increased with maximum change-rate, starts. After the power reaches a steady level of 1.07 pu, it decreases with a pre-defined rate to nominal power again. As with frequency control, the DUT reacts as expected in terms of power. Considering the MHiL internal signals speed reference and actual speed, it is apparent that, again, deviations during the dynamic transitions occur. As with the frequency control before, this is caused by rapid power increase (6 s) and power decrease (15 s), respectively. The root causes are identical to those discussed for Frequency Control. In principle, the MHiL's bandwidth is not high enough to couple the rotor inertia tight enough to the test bench. Compared to the results in the Frequency Control chapter, the observed deviation of the speed signals is much less. This is due to more moderate power change rates compared to the frequency control test.

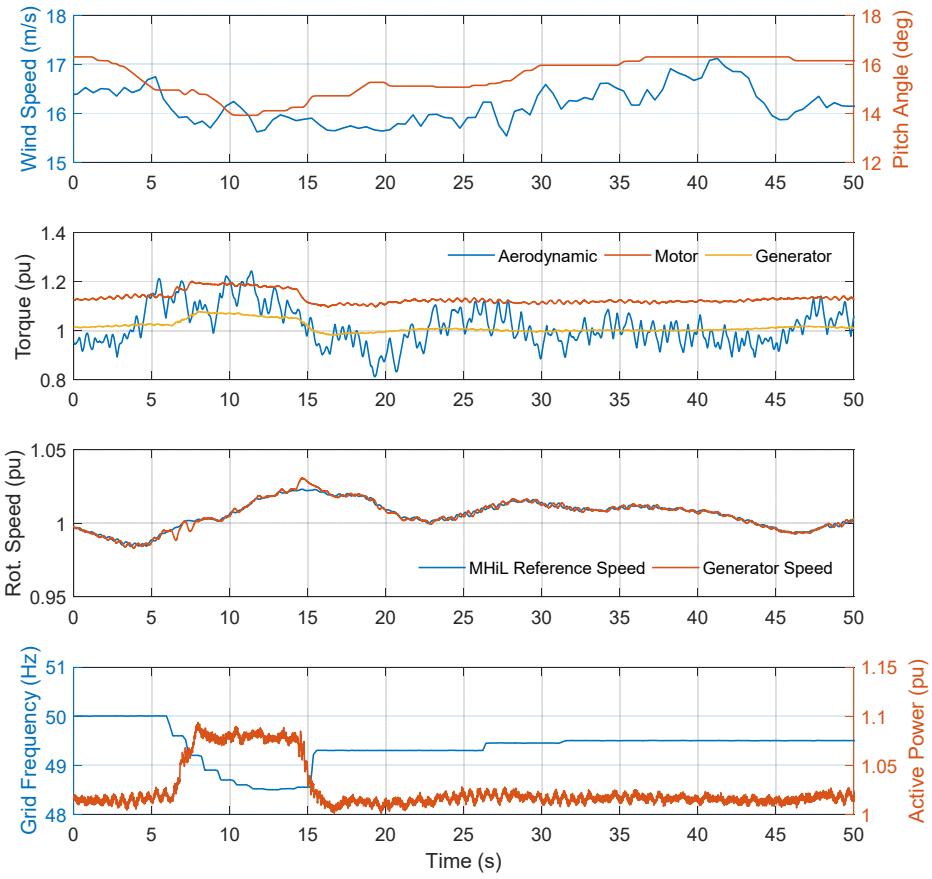

Figure 15. Synthetic inertia test according to IEC61400-21-1.

The effect this difference has on the certification depends on the evaluated quantities. The stationary power boost level, which is evaluated, is not influenced, but reproduced perfectly. In contrast, the dynamic response, in terms of response and settling time, could be influenced. This heavily depends on the gradients set within the DUT software. For the considered DUT, no significant oscillations of the power can be observed so that the settling time is not influenced.

In conclusion, the MHiL system has no negative impact on the measurement results of the synthetic inertia test carried out with this specimen.

6. Discussion and Conclusions

The previous chapters introduced the different HiL systems, which allow operating a wind turbine at a test bench in a realistic manner and carrying out certification measurements. The experimental results showed that, with the given HiL systems, it is possible to conduct certification measurements at the test bench, which lead to results comparable to results from field measurements. As shown in [28], this is not only true for the few tests discussed in this paper, but also for many others and at other nacelle test benches. However, the analysis in this paper also illustrated in detail that a limited accuracy or errors of the HiL systems, their simulation models, and controls could easily compromise the quality of the certification result. In the previous analysis in Section 5, we showed, for instance, that the UVRT results are sensitive to the correct emulation of the impedance by the PHiL, which correlates with the findings in [35], and that, for example, frequency control and synthetic inertia tests can easily be jeopardized by a MHiL system whose bandwidth is limited due to test bench restrictions and poor feedback signals.

Thus, test-bench-based certification is an opportunity for the industry to decrease the time to market, but also carries the risk of a faulty certification if it is not done correctly. Whether the latter happens unknowingly or intentionally, it poses a risk to the entire industry. Standardized procedures for the qualification of a test bench and its HiL systems could help to minimize this risk. Such standard procedures do not yet exist, but need to be developed. Based on the authors' findings in this paper, and experiences from several test bench measurement campaigns, standard tests for several aspects can be proposed.

Models of the grid or parts of the wind turbine, which are implemented in the HiL system, usually contain simplifications and transfer to a different simulation platform. In order to check the validity of these models, the tests recommended to verify the impedance control, dynamic and static test-bench-performance should be used. Beyond that, for the validation of aerodynamic and mechanic models, the final steps of the procedure described in [39] are recommended in order to ensure consistent models.

In order to verify the correctness of the PHiL system impedance control, one should operate the wind turbine at different grid impedances and let the wind turbine feed in a fixed reactive current. The voltage at the PCC should be measured and compared to the theoretical voltage rise/fall at the PCC. Alternatively, UVRT tests can be performed with different grid impedances to verify the correctness of the PHiL system impedance control. For this, one calculates the impedance from the two states before and during the fault, and compares it to the specified value. In both cases, it is important to also consider the impedances of the test setup, such as the DUT transformer. These must be added to the set impedance.

The dynamics of the grid emulator can be specified by performing no-load tests before each UVRT test series and calculating the positive sequence voltage at the PCC for each no-load test. The observed voltage transition should, according to IEC 61400-21-1, last maximum 7.5 ms for the dynamic transition during the dip and 10 ms for the transient voltage transition during recovery [2].

For the verification of the MHiL system's static properties, the DUT can be run at different wind speeds from cut-in to cut-out, with a maximum step size of 1 m/s, in laminar or turbulent conditions. Thereby, each wind speed is held for at least 100 s (laminar) or 600 s (turbulent), respectively. The resulting static values for generator power, rotation

speed, and pitch angle should match results derived in offline simulation. With respect to field results, and also allowing some deviations of different numerical aeroelastic solvers, the tolerable power and speed deviations can be considered up to 0.1 pu. The pitch should be accurate by at least 2°.

For verifying the dynamic performance of the MHiL system and the test bench, different tests are required. In a first test, the DUT operates at different wind speeds from cut-in to cut-out in turbulent conditions. The wind speed steps can be up to 4 m/s. For determining the dynamics, the spectrum of the generator speed or power and is calculated and compared to simulation results of the same test run. For a type 3 wind turbine, a UVRT test can be carried out to determine the dynamics and calculate the spectrum, since the voltage drop leads to a step-like excitement of the mechanical drive train. The difference of the resulting eigenfrequencies should be below 5% of its nominal value, which correlates with tolerances of the mechanical models itself.

The second test, which is required to assess the MHiL system and test bench's dynamic performance is a rapid change of the active power during operation. For this, the maximum change-rate of the active power of the DUT, occurring during operation, is identified. While the DUT is operated at nominal power, the power reference is changed to 0.4 pu, with the identified maximum change rate. The difference of the generator speed between the internal simulation and the experiment should be 2% or less, since higher deviations were found to have a relevant impact on the frequency control results.

The validation steps proposed in the above paragraphs can only be considered as a first draft. Academia and industry are invited to refine and extend this validation procedure with experiences and results derived during test bench measurement campaigns. Ultimately, the national and international standards must include such validation tests and procedures for test benches in order to prevent a lowering of the certification standards and, hence, risking the reputation of a whole industry. Since the goal is to reduce the required DUT hardware and virtualize testing, it is mandatory to define procedures which ensure the capability of a test bench and its HiL systems to serve as a platform for certification.

Important to note at this point is that all experimental results discussed in this paper are based on a type 4 wind turbine. There are no publicly available results for the same test campaign with a type 3 wind turbine. It is very likely that some of the effects regarding the accuracy of the PHiL and the MHiL system are even more important with such a type of wind turbine.

Author Contributions: L.K.: Methodology, Software, Validation, Investigation, Writing—original draft preparation, and Visualization; A.F.: Methodology, Software, Validation, Investigation, Writing—original draft preparation, and Visualization; M.B.: Methodology, Software, Validation, Investigation, and Writing—original draft preparation; U.J.: Conceptualization, Validation, Writing—original draft preparation, Project Administration, and Funding Acquisition; H.R.: Conceptualization, Validation, Writing—review and editing, Project Administration, and Funding Acquisition; T.K.: Writing—review and editing; D.A.: Conceptualization, Writing—review and editing, Resources, and Funding Acquisition; A.M.: Conceptualization, Writing—review and editing, Resources, and Funding Acquisition. All authors have read and agreed to the published version of the manuscript.

Funding: The depicted research is part of the project 'CertBench-Systematic validation of system test benches based on type testing of wind turbines' and funded by the German Federal Ministry of Economic Affairs and Energy (0324200A-E).

Institutional Review Board Statement: Not applicable.

Informed Consent Statement: Not applicable.

Data Availability Statement: Not applicable.

Acknowledgments: The authors would like to thank the project partners of CertBench UL DEWI, FGH Certification, and Fraunhofer IWES for carrying out the project together and supporting the measurement campaign.

Conflicts of Interest: The authors declare no conflict of interest.

Abbreviations

DUT	Device under test
FL	Full load
HiL	Hardware-in-the-Loop
IE	Inertia emulation
ITM	Ideal transformer model
MHiL	Mechanical-level Hardware-in-the-Loop
MRC	Model reference control
PCC	Point of common coupling
PHiL	Power-level Hardware-in-the-Loop
PL	Partial load
UVRT	Under voltage ride through

References

1. Fördergesellschaft Windenergie und andere Erneuerbare Energien. *Technische Richtlinien für Erzeugungseinheiten und -Anlagen Teil 3 (TR3): Bestimmung der Elektrischen Eigenschaften von Erzeugungseinheiten und -Anlagen am Mittel-, Hoch- und Höchstspannungsnetz*, 25th ed. Available online: https://www.hs-albsig.de/fileadmin/user_upload/hsas/01_studienangebot/bachelor/wiw/downloads/Modulhandbuch_WIW_Bachelor_StuPO_19.2_WS_19-20_011020.pdf (accessed on 28 November 2021).
2. International Electrotechnical Commission. *Wind Energy Generation Systems: Part 21-1: Measurement and Assessment of Electrical Characteristics—Wind Turbines*, 1.0 (20 May 2019) ed.; IEC: Geneva, Switzerland, 2019; pp. 27–180.
3. International Electrotechnical Commission. IEC New Work Item Proposal (NP) 88/685/NP: TC 88 Work Programm. Available online: https://www.iec.ch/ords/f?p=103:23:508106504519366::FSP_ORG_ID,FSP_LANG_ID:1282,25 (accessed on 25 November 2021).
4. Riccobono, A.; Helmedag, A.; Berthold, A.; Averous, N.R.; de Doncker, R.W.; Monti, A. Stability and Accuracy Considerations of Power Hardware- in-the-Loop Test Benches for Wind Turbines. *IFAC-PapersOnLine* **2017**, *50*, 10977–10984. [CrossRef]
5. Lauss, G.; Faruque, M.O.; Schoder, K.; Dufour, C.; Viehweider, A.; Langston, J. Characteristics and Design of Power Hardware-in-the-Loop Simulations for Electrical Power Systems. *IEEE Trans. Ind. Electron.* **2016**, *63*, 406–417. [CrossRef]
6. Ren, W.; Steurer, M.; Baldwin, T.L. Improve the Stability and the Accuracy of Power Hardware-in-the-Loop Simulation by Selecting Appropriate Interface Algorithms. *IEEE Trans. Ind. Appl.* **2008**, *44*, 1286–1294. [CrossRef]
7. Siegers, J.; Santi, E. Improved power hardware-in-the-loop interface algorithm using wideband system identification. In Proceedings of the 2014 IEEE Applied Power Electronics Conference and Exposition—APEC 2014, Fort Worth, TX, USA, 16–20 March 2014; pp. 1198–1204, ISBN 978-1-4799-2325-0.
8. Kotsampopoulos, P.; Lagos, D.; Hatziargyriou, N.; Faruque, M.O.; Lauss, G.; Nzimako, O.; Forsyth, P.; Steurer, M.; Ponci, F.; Monti, A.; et al. A Benchmark System for Hardware-in-the-Loop Testing of Distributed Energy Resources. *IEEE Power Energy Technol. Syst. J.* **2018**, *5*, 94–103. [CrossRef]
9. Jassmann, U.; Reiter, M.; Abel, D. An Innovative Method for Rotor Inertia Emulation at Wind Turbine Test Benches. *IFAC Proc. Vol.* **2014**, *47*, 10107–10112. [CrossRef]
10. Schkoda, R.; Bibo, A. A Hardware-in-the-Loop Strategy for Control of a Wind Turbine Test Bench. In Proceedings of the ASME 2015 Dynamic Systems and Control Conference, Columbus, OH, USA, 28 October 2015. V002T21A003.
11. Jassmann, U.; Hakenberg, M.; Abel, D. An extended inertia and eigenfrequency emulation for full-scale wind turbine nacelle test benches. In Proceedings of the 2015 IEEE International Conference on Advanced Intelligent Mechatronics (AIM), Busan, Korea, 7–11 July 2015; pp. 996–1001.
12. Fischer, B.; Jassmann, U. A general framework for a control-based design of power and mechanical hardware-in-the-loop systems. *IFAC-PapersOnLine* **2017**, *50*, 10957–10963. [CrossRef]
13. Neshati, M.; Jersch, T.; Wenske, J. Model based active damping of drive train torsional oscillations for a full-scale wind turbine nacelle test rig. In Proceedings of the 2016 American Control Conference (ACC), Boston, MA, USA, 6–8 July 2016; pp. 2283–2288.
14. Neshati, M.; Zuga, A.; Jersch, T.; Wenske, J. Hardware-in-the-loop Drive Train Control for Realistic Emulation of Rotor Torque in a Full-scale Wind Turbine Nacelle Test Rig. In Proceedings of the 2016 European Control Conference, Aalborg, Denmark, 29 June–1 July 2016; pp. 1481–1486, ISBN 978-1-5090-2590-9.
15. Leisten, C.; Jassmann, U.; Balshüsemann, J.; Hakenberg, M.; Abel, D. Design and Analysis of a MPC-based Mechanical Hardware-in-the-Loop System for Full-Scale Wind Turbine System Test Benches. *IFAC-PapersOnLine* **2017**, *50*, 10985–10991. [CrossRef]
16. Basler, M.; Nguyen, T.A.; Hruschka, F.; Jassmann, U.; Abel, D. A Genetic Algorithm-based Robust Control Approach for Wind Turbine System Test Benches. In Proceedings of the European Control Conference 2020, Saint Petersburg, Russia, 12–15 May 2020; Pogromsky, A., Ebihara, Y., Eds.; IEEE: Piscataway, NJ, USA, 2020; pp. 394–401, ISBN 978-3-90714-402-2.
17. Basler, M.; Hruschka, F.; Abel, D. Robust Linear Parameter-Varying Control for Multi-Megawatt Wind Turbine Testing. In Proceedings of the 60th IEEE Conference on Decision and Control (CDC), Austin, TX, USA, 14–17 December 2021; pp. 2038–2045, ISBN 978-1-6654-3659-5.
18. Fischer, B.; Mehler, C.; Zuga, A.; Shan, M. Control design for mechanical hardware-in-the-loop operation of dynamometers for testing full-scale drive trains. *Wind Energ.* **2016**, *19*, 1889–1901. [CrossRef]

19. Helmedag, A.; Isermann, T.; Monti, A.; Averous, N.R.; Stieneker, M.; de Doncker, R.W. Multi-physics power hardware in the loop test bench for on-shore wind turbine nacelles. In Proceedings of the 2013 IEEE ECCE Asia Downunder, Melbourne, Australia, 3–6 June 2013; pp. 221–226, ISBN 978-1-4799-0482-2.
20. Helmedag, A.; Isermann, T.; Monti, A. Fault Ride Through Certification of Wind Turbines Based on a Hardware in the Loop Setup. *IEEE Trans. Instrum. Meas.* **2014**, *63*, 2312–2321. [CrossRef]
21. Basler, M.; Leisten, C.; Jassmann, U.; Abel, D. Experimental Validation of Inertia-Eigenfrequency Emulation for Wind Turbines on System Test Benches. In Proceedings of the IECON 2020 The 46th Annual Conference of the IEEE Industrial Electronics Society, Singapore, 18–21 October 2020; pp. 205–212, ISBN 978-1-7281-5414-5.
22. Neshati, M.; Wenske, J. Dynamometer Test Rig Drive Train Control with a High Dynamic Performance: Measurements and Experiences. *IFAC-PapersOnLine* **2020**, *53*, 12663–12668. [CrossRef]
23. Azarian, S.; Jersch, T.; Khan, S. Comparison of Impedance Characteristics of Medium Voltage Grid Simulator with LVRT-Container during Symmetrical Voltage Dip. In Proceedings of the 2019 Conference for Wind Power Drives (CWD), Aachen, Germany, 12–13 March 2019.
24. Koralewicz, P.; Gevorgian, V.; Wallen, R.; van der Merwe, W.; Jorg, P. Advanced grid simulator for multi-megawatt power converter testing and certification. In Proceedings of the 2016 IEEE Energy Conversion Congress and Exposition (ECCE), Milwaukee, WI, USA, 18–22 September 2016; IEEE: Piscataway, NJ, USA, 2016; pp. 1–8, ISBN 978-1-5090-0737-0.
25. Koralewicz, P.; Gevorgian, V.; Wallen, R. Multi-megawatt-scale fower-hardware-in-the-loop interface for testing ancillary grid services by converter-coupled generation. In Proceedings of the 2017 IEEE 18th Workshop on Control and Modeling for Power Electronics (COMPEL), Stanford, CA, USA, 9–12 July 2017; IEEE: Piscataway, NJ, USA, 2017; pp. 1–8, ISBN 978-1-5090-5326-1.
26. Helmedag, A.; Isermann, T.; Jassmann, U.; Radner, D.; Abel, D.; Jacobs, G.; Monti, A. Testing nacelles of wind turbines with a hardware in the loop test bench. *IEEE Instrum. Meas. Mag.* **2014**, *17*, 26–33. [CrossRef]
27. Jassmann, U.; Frehn, A.; Kaven, L.; von den Hoff, D.; Röttgers, H.; Frühmann, R.; Santjer, F.; Mehler, C.; Zuga, A.; Quistorf, G.; et al. CertBench—Systematische Validierung von Systemprüfständen Anhand der Typprüfung von Windenergieanlagen: Schlussbericht zum Verbundvorhaben: Berichtszeitraum: 1–31 August 2017, Aachen. 2021. Available online: https://www.tib.eu/de/suchen/id/TIBKAT:1774327848/ (accessed on 28 October 2021).
28. Jassmann, U.; Frehn, A.; Röttgers, H.; Santjer, F.; Mehler, C.; Beißel, T.; Kaven, L.; von den Hoff, D.; Frühmann, R.; Azarian, S.; et al. CertBench: Conclusions from the comparison of certification results derived on system test benches and in the field. *Forsch. Ing.* **2021**, *85*, 353–371. [CrossRef]
29. Neshati, M.; Feja, P.; Zuga, A.; Roettgers, H.; Mendonca, A.; Wenske, J. Hardware-in-the-loop Testing of Wind Turbine Nacelles for Electrical Certification on a Dynamometer Test Rig. In *Journal of Physics: Conference Series*; IOP Publishing: Bristol, UK, 2020; Volume 1618, p. 32042. [CrossRef]
30. Frehn, A.; Azarian, S.; Quistorf, G.; Adloff, S.; Santjer, F.; Monti, A. First comparison of the electrical properties of two grid emulators for UVRT test against field measurement. *Forsch. Ing.* **2021**, *85*, 373–384. [CrossRef]
31. Averous, N.R.; Berthold, A.; Schneider, A.; Schwimmbeck, F.; Monti, A.; de Doncker, R.W. Performance tests of a power-electronics converter for multi-megawatt wind turbines using a grid emulator. In *Journal of Physics: Conference Series*; IOP Publishing: Bristol, UK, 2016; Volume 753, p. 72015. [CrossRef]
32. Bi, L.; Schelenz, R.; Jacobs, G. Dynamic Simulation of Full-Scale Nacelle Test Rig with Focus on Drivetrain Response under Emulated Loads. In Proceedings of the 2nd Conference for Wind Power Drives, Aachen, Germany, 3–4 March 2015.
33. Honrubia-Escribano, A.; Jiménez-Buendía, F.; Sosa-Avendaño, J.L.; Gartmann, P.; Frahm, S.; Fortmann, J.; Sørensen, P.E.; Gómez-Lázaro, E. Fault-Ride Trough Validation of IEC 61400-27-1 Type 3 and Type 4 Models of Different Wind Turbine Manufacturers. *Energies* **2019**, *12*, 3039. [CrossRef]
34. Erlich, I.; Shewarega, F.; Engelhardt, S.; Kretschmann, J.; Fortmann, J. Effect of Wind Turbine Output Current during Faults on Grid Voltage and the Transient Stability of Wind Parks. In Proceedings of the IEEE Power & Energy Society General Meeting, Calgary, AB, Canada, 26–30 July 2009.
35. Frehn, A.; Grune, R.; Röttgers, H.; Monti, A. Influence of the grid parameters during under voltage ride through (UVRT) testing. *Forsch. Ing.* **2021**, *85*, 559–566. [CrossRef]
36. Verband der Elektrotechnik Elektronik Informationstechnik e. V. *VDE-AR-N 4120: Technische Regeln für den Anschluss von Kundenanlagen an das Hochspannungsnetz und Deren Betrieb (TAR Hochspannung)*; VDE e.V.: Offenbach, Germany, 2015.
37. Jassmann, U. Hardware-in-the-Loop Wind Turbine System Test Benches and their Usage for Controller Validation. Ph.D. Thesis, RWTH Aachen University, Aachen, Germany, 2018.
38. Azarian, S.; Jersch, T.; Khan, S. Comparison of impedance behavior of UVRT-Container with medium voltage grid simulator in case of unsymmetrical voltage dip. In Proceedings of the 2019 Conference for Wind Power Drives (CWD), Aachen, Germany, 12–13 March 2019; Abel, D., Ed.; IEEE: Piscataway, NJ, USA, 2019; pp. 1–12, ISBN 978-1-7281-3224-2.
39. Huhn, M.L.; Popko, W. Best practice for verification of wind turbine numerical models. In *Journal of Physics: Conference Series*; IOP Publishing: Bristol, UK, 2020; Volume 1618, p. 52026. [CrossRef]